

Row of Dislocation loops as a Vacancy Source in Ultrahigh-Purity Aluminum Single Crystals with a Low Dislocation Density

Kaoru MIZUNO, Kimihiko MORIKAWA, Hiroyuki OKAMOTO^A
and Eiji HASHIMOTO^B

Department of Materials Science, Shimane University, Matsue 690-8504, Japan
Fax:81-852-32-6409, e-mail:mizuno@riko.shimane-u.ac.jp

^A Department of Health Sciences, Kanazawa University, Kanazawa, 920-0942, Japan
Fax:81-76-234-4360, e-mail:okamoto@mhs.mp.kanazawa-u.ac.jp

^B Hiroshima Synchrotron Radiation Center, Hiroshima University, Higasi-Hiroshima, 730-8511, Japan,
e-mail: ehasimot@hiroshima-u.ac.jp

The vacancy generation process in ultrahigh-purity aluminum single crystals with a low dislocation density was investigated by synchrotron radiation topography using a white X-ray beam. Some straight lines were observed in the topographs taken after temperature rose to 300°C from room temperature, and they were confirmed to be rows of successive small interstitial-type dislocation loops grown as vacancy sources. It was concluded that the thermal generation mechanism of vacancies in ultrahigh-purity aluminum single crystals with a low dislocation density consists of the following two steps. First, small interstitial loops are heterogeneously formed in the crystal lattice; second, these convert to lengthened loops with the development of screw components and finally grow into rows of dislocation loops emitting vacancies into the lattice. However, contribution of new vacancy generation mechanism, growth of row of interstitial type dislocation loop for thermal equilibrium vacancy concentration is less than several percent. Therefore, major vacancy source is small vacancy cluster or vacancy type dislocation loops grown after slow cooling during crystal growth.

Keywords: row of dislocation loops, vacancy source, topography, aluminum

1. Introduction

There are many investigations on the thermal generation of vacancies in metals[1], and it is generally accepted that the predominant source of vacancies in common metal crystals is grown-in dislocation[2]. In nearly perfect crystals with a low dislocation density or dislocation-free crystals, the predominant source for thermally generated vacancies is of interest. We have reported that the predominant vacancy source in aluminum single crystals with a low dislocation density after up-quenching is interstitial-type dislocation loops generated by heterogeneous nucleation[3]. The purity of the aluminum specimen used in this experiment was 99.9999 at % (high purity, 6-N). Therefore, impurities or their clustering may contribute to the nucleation of interstitial loops. Recently, ultrahigh-purity (UHP) aluminum materials (99.9999 at %, 7-N) have become available[4]. Vacancy generation profiles have been investigated by X-ray topography using nearly perfect aluminum single crystals made of UHP materials.

2. Experimental procedure

Aluminum single crystals used in the present investigation were prepared by the strain-annealing method with traveling furnace [5] from zone-refined aluminum in ultra-high vacuum. The residual resistance ratio RRR ($\equiv R_{300K}/R_{4.2K}$) was 1.0×10^4 [6] and the size of the specimens was $0.5 \times 5 \times 50 \text{ mm}^3$. The cooling rate after crystallization at 600°C was 30°C/h down to 400°C, and was 7°C/h below 400°C. Furthermore, the dislocation density of these crystals was decreased by cyclic annealing between 250°C and 150°C with a heating and cooling rate of 25°C/h in vacuum. The final dislocation density determined by Keh's method [7] from the X-ray topographs was decreased to $1 \times 10^3 \text{ cm}^{-2}$. Details of the growth conditions for the specimen and residual dislocation densities have been published elsewhere [8]. Each specimen was mounted in an electric furnace, which was set up on the goniometer of a high-speed X-ray topographic camera (BL-15B1) of the Photon Factory, at the High Energy Accelerator Research Organization (KEK) in Tsukuba, Japan. White beam Laue

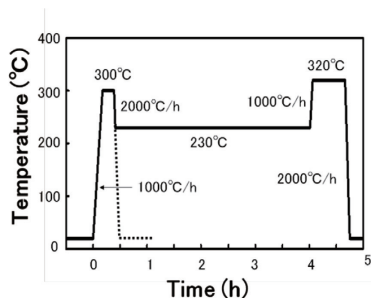


Fig.1 Temperature-time diagram during the topographic observations. The broken line shows the heat treatment for a quenched specimen.

topographs were taken using (111) reflections. The wavelength of the diffracted beam and the exposure time were 0.42 Å and 2.0 s, respectively. All topographs were recorded on Ilford L-4 Nuclear Plates with a 25 μm thick emulsion.

The temperature history during the experiments is shown in Fig. 1. After taking a topograph at room temperature, the temperature of specimen was raised to 300°C in air with a heating rate of 1000°C/h and topographs were then taken at this temperature. The specimen was held at 300°C for 20 min. and was then cooled down to 230°C with a cooling rate of 2000°C/h. Finally, after being held at 230°C for 3.5 hours, the temperature was again raised to 320°C.

3. Experimental results and discussion

3-1. Row of dislocation loops as a vacancy source

Laue topographs by the (111) reflection taken at room temperature (R.T.) and 300°C are shown in Fig. 2 (a) and (b), respectively. A number of black dots are observed in Fig. 2 (b) which was taken after the temperature was raised. These are interstitial-type dislocation loops grown by vacancy sources, as previously reported by the authors for high-purity aluminum crystals [3]. In addition to the black dots,

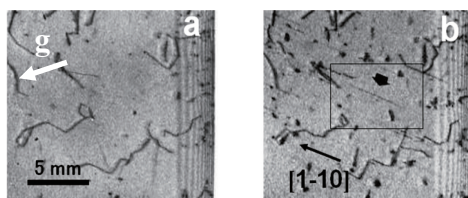


Fig.2 Topographs of an aluminum single crystal specimen taken at (a) R.T. before heating and at (b) 300°C. Some straight lines oriented along <110> are observed in (b) in addition to interstitial-type dislocation loops. An arrow indicates the diffraction vectors, *g*.

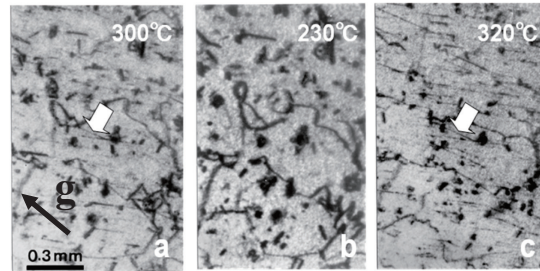


Fig.3 A series of Laue topographs taken at (a) 300°C, (b) 230°C and (c) 320°C after re-heating. The straight lines in (a) and (c) are vacancy sources in ultrahigh-purity aluminum. A black arrow indicates the diffraction vectors, *g*.

long straight-line images can be also seen in Fig. 2 (b). These lines are observed to be always oriented along <110>. Figure 3 (a) shows a topograph taken at 300°C with a different specimen. A number of lines are observed in this figure, similar to Fig. 2 (b). After this topograph was taken, the specimen was cooled to 230°C and held for 3.5 h. Fig. 3(b) shows a topograph taken at the last stage of this annealing step. All the straight lines seen in Fig. 3(a) have disappeared after the cooling down to 230°C. After taking the topograph shown in Fig. 3(b), the specimen temperature was again raised to 320°C and held for 40 min. Figure 3(c) shows the topograph for the specimen after this treatment, taken at 320°C. The straight lines observed at 300°C have reappeared at 320°C. Almost all of the straight lines observed in Fig. 3(a) correspond to those in Fig. 3 (c) as indicated by the arrows showing one example. It is clear that these straight lines appear at the same locations as in the previous heating process. The number density of the straight lines in Fig. 3(a) and (c) are $5 \times 10^2 \text{ cm}^{-2}$ and $1.3 \times 10^3 \text{ cm}^{-2}$, respectively. The number density of the straight lines thus increases with temperature, in other words, thermal equilibrium concentration of vacancies. These must be new vacancy sources instead of the interstitial loops in the nearly perfect crystals. Figure 4 shows a magnified image of the line image in the boxed area in Fig. 2(b). These lines are rows of successive dislocation loops or a lengthened loop with the development of screw components under growth to

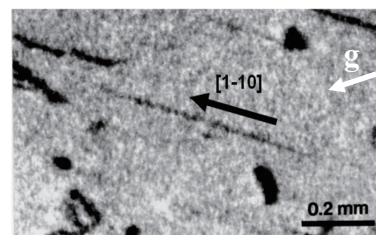


Fig.4 High magnification topograph of the boxed area in Fig.1 (b). The straight lines shown in the previous photographs are dislocation loops in rows grown as vacancy sources. An arrow indicates the diffraction vectors, *g*.

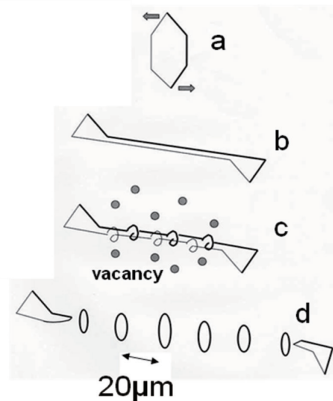


Fig.5 Illustrated representation of the formation mechanism of a row of dislocation loops. (a) Heterogeneously nucleated dislocation loop. (b) Elongation of the loop with development of screw components. (c) Winding up into helical shape of the dislocation with screw character emitting vacancies. (d) Production of new successive loops by intersection of the helices.

a row of loops during emission of vacancies. Based on the above results, these straight lines are determined to be rows of interstitial-type dislocation loops, grown by thermal vacancy sources. The formation of such rows of dislocation loops can be explained as follows. Due to a rapid rise in temperature, a large deficiency of vacancies from the thermal equilibrium concentration occurred. To compensate for this deficiency, vacancies needed to be supplied quickly to the lattice. If the vacancies were supplied only from pre-existing dislocations and the specimen surfaces, it would take a long time for the vacancies to achieve thermal equilibrium over the whole volume of the specimen, because the concentrations of these sources is very low in nearly perfect crystals. In the case of HP aluminum, interstitial dislocation loops were formed heterogeneously in order to supply vacancies. They then grew larger and were imaged as black dots. However, in UHP aluminum, because the low concentration of impurities acts as nucleation centers

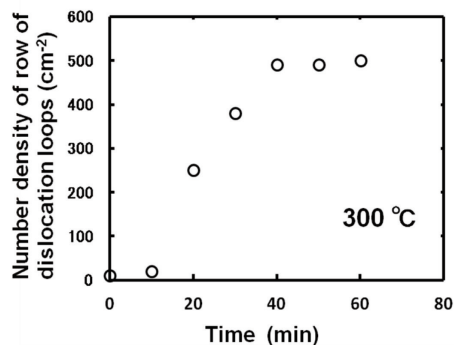


Fig.6 Change of number density of row of dislocation loops after up-quenching.

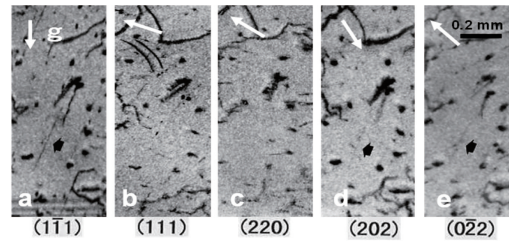


Fig.7 Topographs taken with different diffraction planes. The diffraction planes in (a), (b), (c), (d) and (e) were (1-11), (111), (220), (202) and (0-22), respectively. Arrows indicate the diffraction vectors, g .

for the loops, only a few number of prismatic dislocation loops can nucleate. In order to generate more vacancies, these dislocation loops convert to lengthened loops by the development of screw components, and these screw dislocation parts are able to climb into helical dislocations by emitting vacancies. This ultimately leads to the intersection of parts of the helix with itself, and results in the formation of new closed loops. This mechanism is schematically shown in Fig. 5. Amelinckx and Bontinck have previously proposed a similar growth mechanism of dislocation loops in rows for a vacancy sink [9].

In general, rows of loops are rarely observed in high-purity aluminum single crystals after up-quenching in contrast to interstitial-type dislocation loops. The appearance of many rows of loops acting as vacancy sources was the main feature observed of the UHP aluminum single crystal with a low dislocation density.

Figure 6 shows the change of number density of low of dislocation loops after up-quenching. Total amount of vacancy emitted from the low of dislocation loops at 300 °C was evaluated from the size and the number density. In the calculation, loop diameter and spacing of loops were determined from Fig. 4 and the values were both 20 μm . The calculated amount of vacancy was converted to vacancy concentration, number of vacancies per total number of atoms in unit volume, in order to compare with the contribution of other vacancy sources. Vacancy concentration generated from the row of dislocation loops at 300 °C was 1×10^{-7} . It is about three percent of the thermal equilibrium concentration of vacancy at 300 °C (3×10^{-6}) [10]. Therefore, row of dislocation loops is not dominant vacancy source in UHP aluminum single crystal with a low dislocation density. Major vacancy source is small vacancy cluster or vacancy type dislocation loops grown after slow cooling during crystal growth in a similar way of HP aluminum [8].

3-2. Nature of row of dislocation loops

In order to examine the nature of the row of dislocation loops, we determined the Burgers vector of the dislocation loops consisting the present vacancy source in the quenched specimen, as shown by the broken line in Fig. 1. The Burgers vector was

Table 1 Visibility possibility of the image of a row of dislocation loops from the value of $g \cdot b$.

$g \cdot b$	(111)	($\bar{1}\bar{1}\bar{1}$)	(111)	($2\bar{2}0$)	($0\bar{2}2$)
$a/2[110]$	×	○	○	×	○
$a/2[101]$	○	×	○	○	○
$a/2[011]$	×	×	○	○	×
$a/2[1\bar{1}0]$	○	×	×	○	○
$a/2[10\bar{1}]$	×	○	×	○	○
$a/2[0\bar{1}1]$	○	○	×	○	○

determined by finding the reflection at which a row of loops becomes invisible. Figure 7 shows synchrotron radiation topographs that used white beam X-rays for the same area taken using different diffraction planes. This specimen was quenched from 300°C after the appearance of rows of dislocation loops as vacancy sources. The long row of loops indicated by the arrow is visible in Fig. 7(a), (d) and (e) in contrast to Fig. 7 (b) and (c). In the present case, the possible Burgers vector, b , is of the type $a/2\langle 110 \rangle$ because of the high stacking fault energy in aluminum, where a is the lattice vector. This is the Burgers vector of a perfect dislocation. Table I shows the possibility of visibility of the images obtained from the values of $g \cdot b$ for the dislocation in five 111 and 220 type reflections, i.e. the dislocation is invisible when $g \cdot b = 0$. Comparing the experimental results and Table I, the Burgers vector of the dislocation shown in Fig. 7 was identified to be $a/2[1\bar{1}0]$. This Burgers vector was parallel to the direction of the row of dislocation loops shown in Fig. 7. This also provides clear evidence for the formation mechanism of the rows of dislocation loops proposed in the previous sub-section.

In this paper, we described a new vacancy generation mechanism in UHP aluminum single crystals with a low dislocation density. This process consists of the following three steps: first, small interstitial loops are heterogeneously formed in the crystal lattice; second, these convert to lengthened

loops with the development of screw components, which, via climbing into a helical shape of parallel dislocations with screw components, finally grow into rows of dislocation loops, emitting vacancies into the lattice.

In conclusion, we confirmed the new vacancy generation mechanism in ultrahigh-purity aluminum. The mechanism is growth of successive interstitial-type dislocation loops in row from a heterogeneously grown interstitial-type loop.

Acknowledgement

This work has been performed under the approval of the Photon Factory Advisory Committee (Proposal No. 2011G675).

References:

[1] D. N. Seidman and R. W. Balluffi: Phys. Rev. **139** (1965) A1824.
 [2] F. Higel and R. Seizmann: Crystal Lattice Defects **3** (1972) 13.
 [3] T. Kino and K. Mizuno: J. Phys. Soc. Jpn. **53** (1984) 3290.
 [4] E. Hashimoto and Y. Ueda: Trans. Jpn. Inst. Met. **35** (1994) 262.
 [5] T. Fujiwara and T. Hujita: J. Sci, Hiroshima Univ. **A8** (1938)293.
 [6] Y. Ueda, K. Sakoh and E. Hashimoto: J. Phys. Soc. Jpn. **65** (1996) 3442.
 [7] R. K. Ham, Philos. Mag. **6** (1961)1183.
 [8] K. Mizuno, S. Yamamoto, H. Okamoto, M. Kuga and E. Hashimoto: J. Cryst. Growth **237-239** (2002) 367.
 [9] S. Amelinkx and W. Bontinck: Acta. Metall. **5** (1957) 345.
 [10] K.Ono and T.Kino: J. Phys. Soc. Jpn. **44** (1978) 875.

(Received January 8, 2014; Accepted April 3, 2014)